

CrystEngComm

Accepted Manuscript



This is an *Accepted Manuscript*, which has been through the Royal Society of Chemistry peer review process and has been accepted for publication.

Accepted Manuscripts are published online shortly after acceptance, before technical editing, formatting and proof reading. Using this free service, authors can make their results available to the community, in citable form, before we publish the edited article. We will replace this *Accepted Manuscript* with the edited and formatted *Advance Article* as soon as it is available.

You can find more information about *Accepted Manuscripts* in the [Information for Authors](#).

Please note that technical editing may introduce minor changes to the text and/or graphics, which may alter content. The journal's standard [Terms & Conditions](#) and the [Ethical guidelines](#) still apply. In no event shall the Royal Society of Chemistry be held responsible for any errors or omissions in this *Accepted Manuscript* or any consequences arising from the use of any information it contains.

Cite this: DOI: 10.1039/c0xx00000x

www.rsc.org/xxxxxx

ARTICLE TYPE

Syntheses, crystal structures and properties of inorganic-organic hybrids constructed from Keggin-type polyoxometalates and silver coordination compounds†

Wei-Li Zhou,^a Jun Liang,^a Chao Qin,^{*a} Kui-Zhan Shao,^a Fang-Ming Wang^{*b} and Zhong-Min Su^{*a}⁵ Received (in XXX, XXX) Xth XXXXXXXXX 20XX, Accepted Xth XXXXXXXXX 20XX

DOI: 10.1039/b000000x

Four inorganic-organic hybrids based on polyoxometalates (POMs), [Ag₄(btz)₂(Hbtz)₂(H₂O)Na(PMo₁₂O₄₀)·H₂O] (**1**), [Ag₂(4,4'-bpy)₂Ag₂(4,4'-bpy)(H₂O)₂(PMo^{VI}Mo₁₁O₄₀)] (**2**), [Ag₅(btz)₂(4,4'-bpy)₂(PMo₁₂O₄₀)·3H₂O] (**3**), and [Ag₅(btz)₂(4,4'-bpy)₂(PW₁₂O₄₀)·3H₂O] (**4**) (Hbtz = 1-H-1,2,3-benzotriazole, 4,4'-bpy = 4,4'-bipyridine) have been hydrothermally synthesized and structurally characterized by conventional techniques. Compound **1** is a 2D layer composed of Ag^I ions, btz ligands and [PMo₁₂O₄₀]³⁻ anions. While compound **2** represents a rare 3D poly-threading framework based on infinite 2D layers made up of {POM–Ag₂} inorganic building blocks and bpy ligands, which were threaded by silver-organic linear double chains. Compounds **3** and **4** are iso-structural and exhibit three-fold interpenetrating diamondoid frameworks containing tri-nuclear silver centers as nodes and hexa-nuclear silver-organic macro-cycles and [PMo₁₂O₄₀]³⁻ anions, both as bi-connected units. Furthermore, their electrochemical properties, fluorescence properties and optical band gaps have been investigated in detail.

Introduction

Polyoxometalates (POMs), as an important family of metal oxides, have long been of intense scientific and technological interest, particularly in the field of catalysis, electrochemistry, magnetism, and medicine.¹ Benefiting from their high charge, large size and many surface oxygen atoms, POMs can act as a versatile ligand to coordinate with various transition metal ions or as anion template to direct the assemblies of metal poly-nuclear clusters with fascinating geometry and connectivity.² During the last few decades, design and assembly of inorganic-organic hybrids based on the POMs and transition metal coordination fragments have attracted substantial attention because of their structural diversities and potential applications as functional materials.³ Up to now, there have been reports of interesting 1-, 2- and 3-periodic crystalline lattices based on the Keggin heteropolyanions as linkers,⁴ but it still remains an intriguing challenge to construct high-dimensional POMs-based frameworks, especially with poly-nuclear metal clusters.

Recently, how to construct high-nuclearity clusters and high-dimensional POMs-based hybrids aroused our research interest. The well known Keggin cluster [PMo₁₂O₄₀]³⁻ and [PW₁₂O₄₀]³⁻ (abbreviated to {PMo₁₂} and {PW₁₂}) are chosen as the building block due to their facile preparation and relative stability.⁵ On the other hand, Ag(I), as a d¹⁰ transition metal cation, possesses high affinity for N and O donors and has versatile coordination ability under hydrothermal conditions, which might facilitate the formation of 3D structures.⁶ Besides, Ag^I ions can commonly

form argentophilic Ag-Ag interactions, which lead to the formation of polynuclear silver complexes.⁷ The variety of POMs-based hybrid compounds have showed that N-heterocycle ligands are promising candidates for their different steric effect, soft-rigid degree, and varied geometry in the formation of complexes.⁸ Recent studies have indicated that 1-H-1,2,3-benzotriazole (Hbtz) ligands tend to interconnect metal ions through adjacent N atoms to supply polynuclear complexes with unique structures, but supramolecules and low-dimensional compounds are usually the frustrating results.⁹ We envision that the introduction of auxiliary ligands as a linker might be helpful to obtain high-dimensional POMs-based hybrids. Neutral 4,4'-bipyridine has proved to be an excellent bi-topic bridging ligand and can form 'scaffolding-like materials' using proper metal centers. In fact, a few of 3D compounds were achieved by the use of this pillar ligand, which is prone to form infinite structures.¹⁰

Herein, we chose multifunctional N-heterocycle ligands 1-H-1,2,3-benzotriazole (Hbtz) or (and) 4,4'-bipyridine as well as Ag ions to investigate the effect of mixed ligands on the formation of POMs-based hybrids. Four novel inorganic-organic hybrids based on Keggin-type POMs, [Ag₄(btz)₂(Hbtz)₂(H₂O)Na(PMo₁₂O₄₀)·H₂O] (**1**), [Ag₂(4,4'-bpy)₂Ag₂(4,4'-bpy)(H₂O)₂(PMo^{VI}Mo₁₁O₄₀)] (**2**), [Ag₅(btz)₂(4,4'-bpy)₂(PMo₁₂O₄₀)·3H₂O] (**3**), and [Ag₅(btz)₂(4,4'-bpy)₂(PW₁₂O₄₀)·3H₂O] (**4**) have been successfully obtained. In compound **1**, the combination of Ag^I ions, btz and [PMo₁₂O₄₀]³⁻ anions leads to a 2D layer. Compound **2** possesses a 3D poly-

threading framework containing {Ag-(4,4'-bpy)} chains and {POM-Ag₂}-bpy layers. Compounds **3** and **4** are iso-structural and exhibit three-fold interpenetrating diamondoid 3D frameworks. The electrochemical properties, fluorescence

properties and optical band gaps of **1–3** have been investigated.

Experimental

Materials and methods

Table 1 Crystal Data and Structure Refinement for **1–4**

| Compound | 1 | 2 | 3 | 4 |
|--|---|--|---|--|
| Empirical formula | C ₂₄ H ₂₂ Ag ₄ N ₁₂ NaO ₄₂ PMo ₁₂ | C ₃₀ H ₂₈ Ag ₄ N ₆ O ₄₂ PMo ₁₂ | C ₃₂ H ₃₀ Ag ₅ N ₁₀ O ₄₃ PMo ₁₂ | C ₃₂ H ₃₀ Ag ₅ N ₁₀ O ₄₃ PW ₁₂ |
| <i>M</i> | 2787.26 | 2758.31 | 2964.26 | 4019.18 |
| <i>T</i> /K | 293(2) | 293(2) | 298(2) | 293(2) |
| Crystal system | Monoclinic | Triclinic | Monoclinic | Monoclinic |
| Space group | <i>P</i> 2 ₁ / <i>n</i> | <i>P</i> -1 | <i>C</i> 2/ <i>c</i> | <i>C</i> 2/ <i>c</i> |
| <i>a</i> /Å | 12.977(5) | 11.396(5) | 23.049(5) | 22.902(5) |
| <i>b</i> /Å | 20.255(5) | 11.792(5) | 11.765(5) | 11.913(5) |
| <i>c</i> /Å | 21.995(5) | 13.376(5) | 22.522(5) | 22.594(5) |
| <i>α</i> /° | 90.000(5) | 65.249(5) | 90.000(5) | 90.000(5) |
| <i>β</i> /° | 97.708(5) | 80.299(5) | 101.828(5) | 101.657(5) |
| <i>γ</i> /° | 90.000(5) | 61.303(5) | 90.000(5) | 90.000(5) |
| <i>V</i> /Å ³ | 5729(3) | 1430.7(10) | 5978(3) | 6037(3) |
| <i>Z</i> | 4 | 1 | 4 | 4 |
| <i>D_c</i> /Mg m ⁻³ | 3.231 | 3.202 | 3.294 | 4.422 |
| Measured reflections | 28995 | 7326 | 14374 | 14776 |
| Independent reflections | 10055 | 4918 | 5245 | 5313 |
| <i>R_{int}</i> | 0.0316 | 0.0215 | 0.0630 | 0.0624 |
| <i>R₁</i> (<i>I</i> > 2σ(<i>I</i>)) ^a | 0.0265 | 0.0385 | 0.0448 | 0.0548 |
| <i>wR₂</i> (all data) ^a | 0.0553 | 0.0901 | 0.1026 | 0.1207 |
| Goodness-of-fit on <i>F</i> ² | 1.004 | 1.083 | 1.055 | 1.093 |

^a $R_1 = \sum ||F_o| - |F_c|| / \sum |F_o|$. ^b $wR_2 = \sqrt{\sum w(|F_o|^2 - |F_c|^2)|^2} / \sum w(F_o^2)^{1/2}$

All reagents for synthesis were purchased from commercial sources and used without further purification. Elemental analyses (C, H, and N) were performed on a Perkin-Elmer 2400 CHN elemental analyzer; Ag, P, Na and Mo were determined with a Plasma-SPEC(I) ICP atomic emission spectrometer. The Fourier transform infrared (FT-IR) spectra were recorded from KBr pellets in the range 4000–400 cm⁻¹ on an Alpha-Centauri spectrometer. XRPD patterns were collected on a Rigaku D/max-II B X-ray diffractometer with graphite monochromatized Cu Kα radiation (λ = 1.5418 Å) and 2θ ranging from 5 to 50°. Solid state luminescent spectra were measured on a Cary Eclipse spectrofluorometer (Varian) equipped with a xenon lamp and quartz carrier at room temperature. The solid state UV-vis absorption spectra were taken on a Cary 500 spectrophotometer. Thermogravimetric analysis (TGA) was performed on a Perkin-Elmer TG-7 analyzer heated from 20 to 800 °C under nitrogen. A CHI 440 electrochemical workstation connected to a Digital-586 personal computer was used for control of the electrochemical measurements and for data collection.

X-Ray crystallography

Single-crystal X-ray diffraction data for **1–4** were recorded on a Bruker Apex CCD II area-detector diffractometer with graphite-monochromated MoKα radiation (λ=0.71069 Å) at 293(2) K. Absorption corrections were applied using multiscan technique and performed by using the SADABS program. The structures of **1–4** were solved by direct methods and refined on *F*² by full-matrix leastsquares methods by using the SHELXTL package. The crystal data and structure refinement results of **1–4** are

summarized in Table 1. CCDC 988327 (**1**), 988328 (**2**), 988326 (**3**) and 988329 (**4**) contain the supplementary crystallographic data for this paper. In compound **2**, the central P1 atom of the {PMo₁₂} moiety lies on an inversion centre, with concomitant disorder of the four oxygens bonded to it, and also that bpy ligand bonded to Ag1 lies about another independent inversion centre. In compound **3**, the Ag3 atom lies on a twofold axis and that the central P1 atom of the {PMo₁₂} moiety lies on an inversion centre, with concomitant disorder of the four oxygens bonded to it. These data can be obtained free of charge from the Cambridge Crystallographic Data Centre via www.ccdc.cam.ac.uk/data_request/cif.

Preparation of compounds **1–4**

Synthesis of [Ag₄(btz)₂(Hbtz)₂(H₂O)Na(PMo₁₂O₄₀)·H₂O] (**1**).

A mixture of H₃PMo₁₂O₄₀·12H₂O (0.051 g, 0.025 mmol), Ag(CH₃CO₂) (0.034 g, 0.1 mmol), Hbtz (0.024 g, 0.1 mmol) and H₂O (8 mL) was stirred for 0.5 h in air. The pH value of the mixture was adjusted to 3.0 with 1.0 mol L⁻¹ NaOH, then the mixture was transferred to a Teflon-lined reactor and kept under auto-genous pressure at 160 °C for 4 days. After the autoclave was slowly cooled to room temperature at the rate of 10 °C h⁻¹, dark orange block crystals of **1** were obtained. The crystals were filtered, washed with distilled water and dried at room temperature (0.025 g, 35% yield based on Ag). Anal. Calc. for C₂₄H₂₂Ag₄N₁₂NaO₄₂PMo₁₂ (2787.26): Ag, 15.50; P, 1.11; Mo, 41.33; C, 10.33; H, 0.79; Na, 0.83; N, 6.03%. Found: Ag, 15.55; P, 1.13; Mo, 41.39; C, 10.38; H, 0.81; Na, 0.85; N, 6.08%. IR (KBr, cm⁻¹): 3500 (w), 1593 (w), 1219 (m), 1185 (m), 1143 (w),

1058 (s), 954 (s), 876 (s), 796 (s).

Synthesis of $[\text{Ag}_2(4,4'\text{-bpy})_2\text{Ag}_2(4,4'\text{-bpy})(\text{H}_2\text{O})_2(\text{PMo}^{\text{VI}}\text{Mo}^{\text{VI}}\text{O}_{40})]$ (2). A mixture of $\text{H}_3\text{PMo}_{12}\text{O}_{40} \cdot 12\text{H}_2\text{O}$ (0.051 g, 0.025 mmol), $\text{Ag}(\text{CH}_3\text{CO}_2)$ (0.034 g, 0.1 mmol), 4,4'-bpy (0.023 g, 0.075 mmol) and H_2O (8 mL) was stirred for 0.5 h in air. The pH value of the mixture was adjusted to 2.0 with 1.0 mol L^{-1} NaOH, then transferred to a Teflon-lined reactor and kept under auto-genous pressure at $160 \text{ }^\circ\text{C}$ for 4 days. After the autoclave was slowly cooled to room temperature at the rate of $10 \text{ }^\circ\text{C h}^{-1}$, black block crystals of **2** were obtained. The crystals were filtered, washed with distilled water and dried at room temperature (0.021 g, 30% yield based on Ag). Anal. Calc. for $\text{C}_{30}\text{H}_{28}\text{Ag}_4\text{N}_6\text{O}_{42}\text{PMo}_{12}$ (2758.31): Ag, 15.66; P, 1.12; Mo, 41.76; C, 13.05; H, 1.02; N, 3.05%. Found: Ag, 15.69; P, 1.15; Mo, 41.81; C, 13.03; H, 1.09; N, 3.08%. IR (KBr, cm^{-1}): 3503 (w), 1605 (m), 1530 (w), 1486 (m), 1415 (m), 1200 (w), 1058 (s), 954 (s), 869 (s), 791 (s).

Synthesis of $[\text{Ag}_5(\text{btz})_2(4,4'\text{-bpy})_2(\text{PMo}_{12}\text{O}_{40}) \cdot 3\text{H}_2\text{O}]$ (3). A mixture of $\text{Ag}(\text{CH}_3\text{CO}_2)$ (0.042g, 0.125mmol), Hbtz (0.012g, 0.05mmol), 4,4'-bpy (0.015g, 0.05mmol) and H_2O (8 mL) was stirred for 0.5 h in air, then $\text{H}_3\text{PMo}_{12}\text{O}_{40} \cdot 12\text{H}_2\text{O}$ (0.051 g, 0.025 mmol) was added to the mixture. The pH value of the mixture was adjusted to 2.5 with 1.0 mol L^{-1} NaOH, finally transferred to a Teflon-lined reactor and kept under auto-genous pressure at $160 \text{ }^\circ\text{C}$ for 4 days. After the autoclave was slowly cooled to room temperature at the rate of $10 \text{ }^\circ\text{C h}^{-1}$, red block crystals of **3** were obtained. The crystals were filtered, washed with distilled water and dried at room temperature (0.030 g, 40% yield based on Ag). Anal. Calc. for $\text{C}_{32}\text{H}_{30}\text{Ag}_5\text{N}_{10}\text{O}_{43}\text{PMo}_{12}$ (2964.26): Ag, 18.22; P, 1.05; Mo, 38.84; C, 12.95; H, 1.01; N, 4.72%. Found: Ag, 18.21; P, 1.06; Mo, 38.86; C, 12.99; H, 1.05; N, 4.74%. IR (KBr, cm^{-1}): 3445 (m), 1601 (m), 1528 (w), 1489 (w), 1414 (m), 1221 (w), 1186 (m), 1165 (w), 1061 (s), 946 (s), 869 (s), 798 (s).

Synthesis of $[\text{Ag}_5(\text{btz})_2(4,4'\text{-bpy})_2(\text{PW}_{12}\text{O}_{40}) \cdot 3\text{H}_2\text{O}]$ (4). The synthesis method of **4** is similar to that of **3** except for $\text{H}_3\text{PW}_{12}\text{O}_{40} \cdot 12\text{H}_2\text{O}$ (0.077 g, 0.025 mmol) as the substitute of $\text{H}_3\text{PMo}_{12}\text{O}_{40} \cdot 12\text{H}_2\text{O}$. Yellow block crystals of **4** were obtained. The crystals were filtered, washed with distilled water and dried at room temperature (0.035 g, 35% yield based on Ag). Anal. Calc. for $\text{C}_{32}\text{H}_{30}\text{Ag}_5\text{N}_{10}\text{O}_{43}\text{PW}_{12}$ (4019.18): Ag, 13.42; P, 0.77; W, 54.89; C, 9.56; H, 0.75; N, 3.48%. Found: Ag, 13.46; P, 0.75; W, 54.94; C, 9.55; H, 0.76; N, 3.47%. IR (KBr, cm^{-1}): 1601 (m), 1526 (w), 1485 (w), 1415 (m), 1221 (w), 1188 (w), 1165 (m), 1083 (s), 972 (s), 893 (s), 804 (s).

Preparations of 1–4 CPEs. Compounds **1–4** modified carbon paste electrodes **1-CPE**, **2-CPE**, **3-CPE** and **4-CPE** were prepared as follows: 90 mg of graphite powder and 10 mg of compounds **1–4** were mixed and ground together by agate mortar and pestle to achieve a uniform mixture, and then 0.6 mL nujol was added with stirring. The homogenized mixture was used to pack 3 mm inner diameter glass tubes to a length of 0.8 cm. The tube surface was wiped with weighing paper, and the electrical contact was established with the copper stick through the back of the electrode.

Results and discussion

Synthesis

Ag ions are used in the syntheses of all four compounds. Compound **1** and **2** are based on single ligand (btz and 4,4'-pyridine, respectively), while compounds **3** and **4** are iso-structural and both are based on mixed ligands mentioned above. Many parallel experiments were performed by changing the pH of the system in order to investigate the influence of the pH on the final crystal structure. The experimental results show that pH value is an important factor on the final products. As for the syntheses of compounds **1**, **2** and **3**, the pH range of 2–3 is proved to be rational. When the pH is higher than 3.0, only precipitates can be obtained. For compound **4**, the reasonable pH value range changed from 2 to 5 when the $\{\text{PW}_{12}\}$ was used as the reactant.

In addition, another important factor in the construction of the title compounds is the molar ratio of POM-Ag-ligand. The parallel experiments show that the appropriate molar ratios are approximately 1 : 4 : 4 for **1**, 1 : 4 : 3 for **2**, and 1 : 5 : 2 : 2 for **3** and **4**, respectively. When the molar ratio of reactants was changed, the quality of crystals also reduced and even no products could be achieved. Therefore, a proper ratio of the reactants is also a necessary condition for synthesis of the above compounds.

In a word, in the case of fixed reaction temperature, reasonable pH value, the suitable ligands and proper ratio of the reactants are very important in the synthetic reaction of POM-Ag^I compounds.

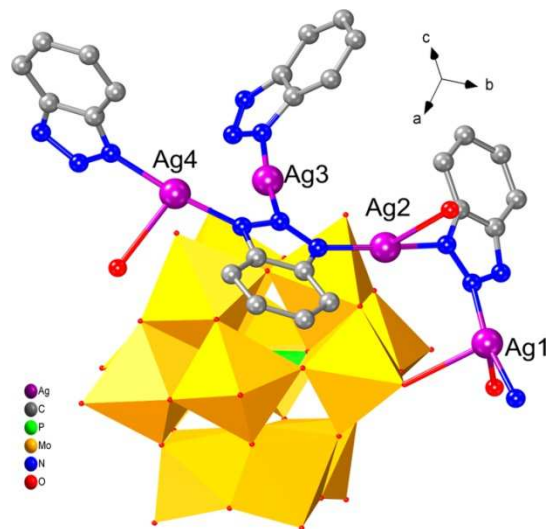


Fig. 1 Ball/stick and polyhedral view of the coordination fashions of the $[\text{PMo}_{12}\text{O}_{40}]^{3-}$ polyoxoanion and Ag^{I} ions in compound **1**. The hydrogen atoms and crystal water molecules are omitted for clarity.

Structure description of $[\text{Ag}_4(\text{btz})_2(\text{Hbtz})_2(\text{H}_2\text{O})\text{Na}(\text{PMo}_{12}\text{O}_{40}) \cdot \text{H}_2\text{O}]$ (1). Single-crystal X-ray diffraction analysis reveals that the asymmetric unit of compound **1** consists of four Ag^{I} ions, one Na ion, two btz anions, two Hbtz ligands, one Keggin-type $\{\text{PMo}_{12}\}$ cluster, one coordinated water molecule and one lattice water molecule (Fig. 1). The valence sum calculations show that all of the Mo atoms are in the +VI oxidation state and Ag atoms are in the +I oxidation state.

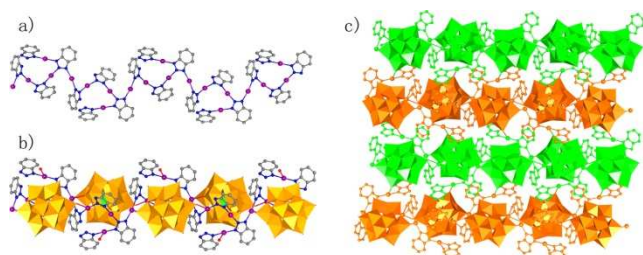


Fig. 2 (a) 1D chain constructed from Ag^{I} ions and btz ligands. (b) 1D chain constructed from Ag^{I} ions, btz ligands and $[\text{PMo}_{12}\text{O}_{40}]^{3-}$ anions. (c) 2D layer constructed by the 1D chains. The adjacent chains were painted in different colors for clarity. The hydrogen atoms and crystal water molecules are omitted for clarity.

The $\{\text{PMo}_{12}\}$ anion, acting as a three-connected inorganic ligand, offers two terminal oxygen atoms (O1 and O2) and one bridging oxygen atom (O5) to coordinate with three crystallographically independent Ag^{I} ions (Ag1, Ag2 and Ag4). While each Ag1 ion is four-coordinated in a ‘seesaw’ configuration by one terminal O atom (O2) from $\{\text{PMo}_{12}\}$ anion, one O atom from one coordinated water molecule (O1W) and two N donors (N1 and N11) from two Hbtz ligands. The Ag2 ion shows a three-coordinated configuration $\{\text{AgN}_2\text{O}\}$, completed by one bridging O (O5) from $\{\text{PMo}_{12}\}$ anion and two N donors (N2 and N3) from two Hbtz ligands. The Ag3 ion adopts a two-coordinated pattern and shows a linear coordination geometry $\{\text{AgN}_2\}$, which is completed by two N atoms (N4 and N10) from two Hbtz ligands. The Ag4 ion connects with two N atoms (N5 and N7) from two Hbtz ligands and one terminal O atom (O1) from $\{\text{PMo}_{12}\}$ anion in a ‘T’-type geometry $\{\text{AgN}_2\text{O}\}$. The bond distances and angles around the Ag^{I} ions are 2.10(5)–2.23(6) Å for Ag–N bonds and 2.44(5)–2.67(9) Å for Ag–O bonds, while the N–Ag–N angle range is in 170.12(16)–173.40(14)°.

Different from the chair-like heptanuclear silver complex,¹¹ the four btz ligands show three types of conformation modes: μ_1 -, μ_2 - and μ_3 - coordination modes in compound **1**. As shown in Fig. 2a, the combination of Ag^{I} ions and btz ligands fabricates 1D wavy chains, in which $[\text{PMo}_{12}\text{O}_{40}]^{3-}$ anions are connected by Ag1 and Ag2 ions to construct a chainlike infinite structure (Fig. 2b). Each 1D chain connects adjacent chain by shearing Ag4 ions, thus forming a 2D layer (Fig. 2c). These 2-D layers are further stacked into a novel 3-D supramolecular structure (Fig. S1).

Structure description of $[\text{Ag}_2(4,4'\text{-bpy})_2\text{Ag}_2(4,4'\text{-bpy})(\text{H}_2\text{O})_2(\text{PMo}^{\text{V}}\text{Mo}^{\text{VI}}_{11}\text{O}_{40})]$ (2**).** Crystal structure analysis reveals that compound **2** consists of four Ag^{I} ions, three 4,4'-bpy ligands, two coordinated water molecules and one Keggin-type $\{\text{PMo}_{12}\}$ cluster (Fig. 3). The $\{\text{PMo}_{12}\}$ anion represents a classical α -Keggin configuration with P center surrounded by a cube of eight disordered oxygen atoms, with each oxygen site half-occupied.¹² The XPS spectrum (Fig. S2), the valence sum calculations and charge balance of the empirical formula show that one of Mo atoms of $\{\text{PMo}_{12}\}$ anion is in the +V oxidation state and Ag atoms are in the +I oxidation state.¹³ The crystal color can also prove that the molybdenum atom is reduced.¹⁴

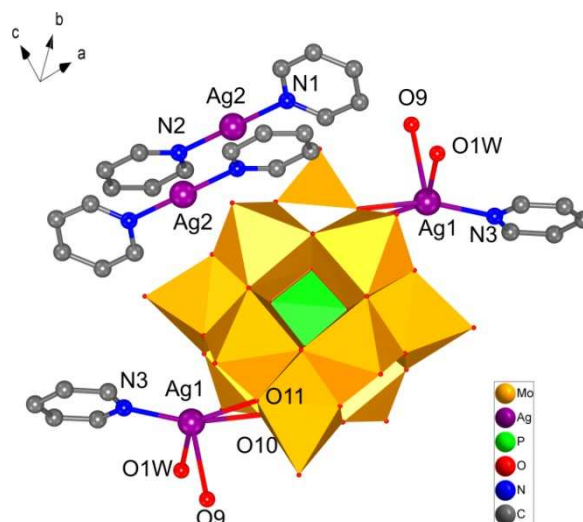


Fig. 3 Ball/stick and polyhedral view of the coordination fashions of the PMo_{12} polyoxoanion and Ag^{I} ions in compound **2**. The hydrogen atoms and crystal water molecules are omitted for clarity.

There are two crystallographically independent Ag^{I} ions (Ag1 and Ag2) in compound **2** which are different from the compound reported by Chen's group in 2006.¹⁵ Although both compounds contain infinite inorganic Ag-POMs polymer chains and infinite Ag-bpy chains, their structures were significantly different. The Ag1 ion is five-coordinated in a distorted trigonal bipyramidal geometry, coordinated by one N atom (N3) from 4,4'-bpy, one O atom from coordinated water molecule (O1W), two bridging O atom (O10, O11) located at the ‘cap’ site of one $\{\text{PMo}_{12}\}$ anion and one terminal O atom (O9) from another $\{\text{PMo}_{12}\}$ anion. The bond distances around the Ag1 ions are 2.22(6) Å for Ag–N bonds and 2.44(11)–2.56(7) Å for Ag–O bonds. The Ag2 ion is coordinated by two N atoms (N1, N2) from two separate 4,4'-bpy ligands. The bond distances and angles around the Ag2 ions are 2.16(9)–2.17(10) Å for Ag–N bonds, while the N–Ag–N angle is 178.87(25)°.

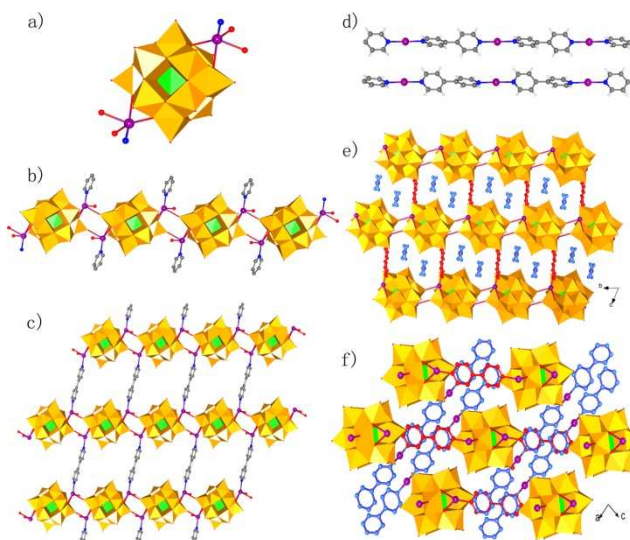


Fig. 4 (a) View of the bicapped-POM cluster. (b) 1D chain constructed from bicapped-POM clusters by sharing terminal oxygen atoms. (c) Representation of the grid-like 2D layer in **2**. (d) View of silver-organic infinite double chains. (e) The 3D poly-threading POM-based framework in compound **2** view along the *a* axis and (f) along the *b* axis (4,4'-bpys in 2D layers (red); 4,4'-bpys in chains (blue)).

Compound **2** represents a rare 1D+2D → 3D poly-threading framework based on infinite 2D layers made up of {POM–Ag₂} inorganic building blocks and 4,4'-bipyridine, which were threaded by silver-organic linear double chains. To understand fully, we shall describe by step. As displayed in Fig. 4a, first of all, the bicapped-POM cluster can be described as a classical α -Keggin core with two five-coordinated silver atoms capping two opposite pits. Each bicapped-POM cluster connects adjacent clusters by shearing terminal oxygen atoms, thus forming a 1D inorganic chain structure (Fig. 4b). Further, 4,4'-bpy ligands bridge adjacent chains to form a flat 2D layer by coordinating with two capped silver metal centers (Fig. 4c). It should be noted that the void in these parallelogram 2D layers (about 11.49 × 11.79 Å²) is just large enough to accommodate a pair of 4,4'-bpy ligands (Fig. 4d, 4e). Remarkably, this is satisfied by the infinite straight double chains with repeated [Ag–4,4'-bpy] units (Fig. 4f). As a result, a poly-threading POM-based framework was well constructed from parallel parallelogram 2D layers threaded by infinite straight double-chains (Fig. 5).

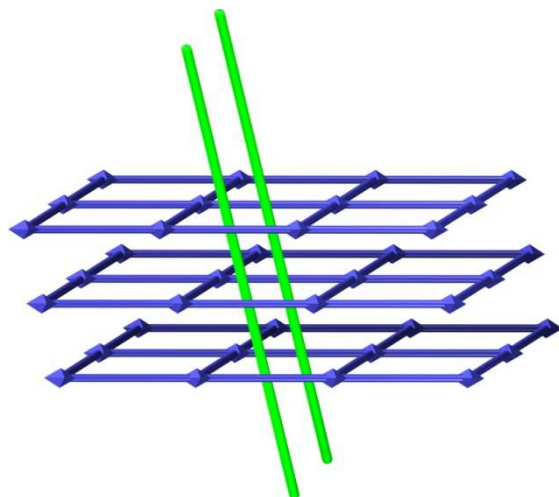


Fig. 5 Schematic view of the 3D poly-threading POM-based framework in compound **2** (blue parallelogram framework, {POM–Ag–4,4'-bpy} layer; green rod, {Ag–4,4'-bpy} chain; blue polyhedron, bicapped POMs).

Structure description of [Ag₅(btz)₂(4,4'-bpy)₂(PMo₁₂O₄₀)·3H₂O] (3**) and [Ag₅(btz)₂(4,4'-bpy)₂(PW₁₂O₄₀)·3H₂O] (**4**).** The single crystal X-ray diffraction analyses reveal that compound **3** and **4** are isomorphous and isostructural, the unit cell dimensions, volumes, related bond distances and angles are only slightly changed. Here, we only discuss in detail the structure and properties of compound **3**. It consists of one Keggin-type {PMo₁₂} cluster, five Ag^I ions, two btz anions, two 4,4'-bpy ligands and three free water molecules

(Fig. 6). The {PMo₁₂} anion shows a classical α -Keggin configuration. The central atom P is disorderly surrounded by a cube of eight oxygen atoms, with each oxygen site half-occupied.

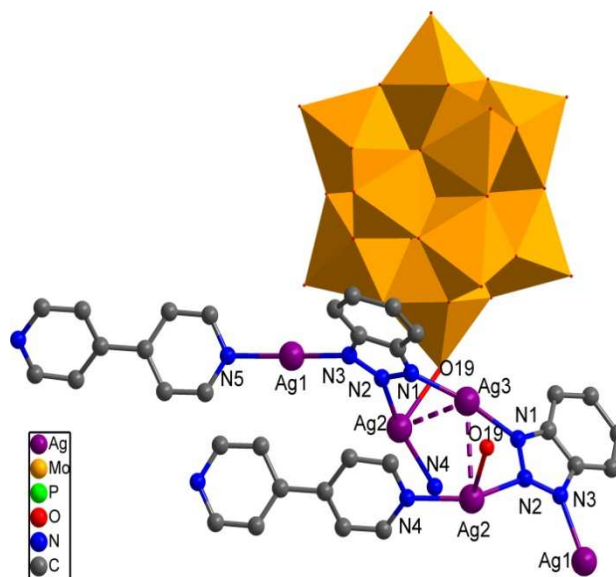


Fig. 6 Ball/stick and polyhedral view of the coordination fashions of the PMo₁₂ polyoxoanion and Ag^I ions in compound **3**. The hydrogen atoms and crystal water molecules are omitted for clarity. Dashed lines: Ag...Ag interaction.

The three crystallographically independent silver atoms (Ag1, Ag2 and Ag3) exhibit two sorts of coordination geometries: bi-coordinated Ag1 and Ag3, and tri-coordinated Ag2. The Ag1 achieves its linear geometry {AgN₂} by coordinating with two N atoms of one btz anion and one 4,4'-bpy ligand. Each Ag2 ion resides in a “T-type” mode {AgN₂O}, coordinated by one btz anion, one 4,4'-bpy and one terminal O atom (O19) located at the ‘cap’ site of the {PMo₁₂} anion. While Ag3 adopts linear geometry coordinated by two nitrogen atoms from two separated

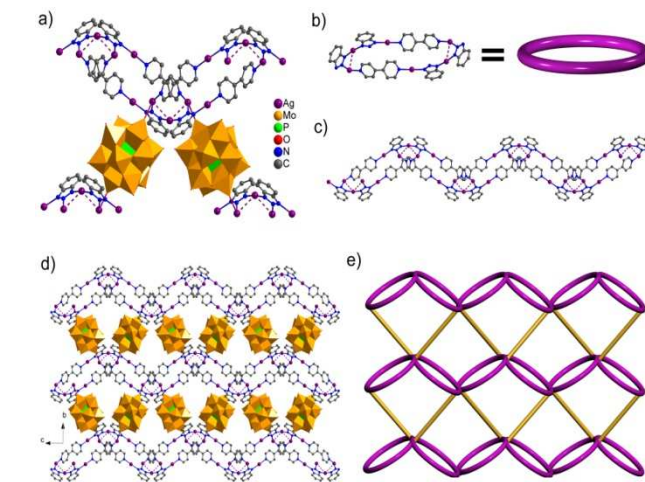


Fig. 7 (a) Chemical view of the basic repeated unit containing (b) the hexa-nuclear silver-organic loop in **3**. (c) The 1D wave chain based on the hexa-nuclear loops. (d) The polyhedral and ball-and-stick representation and (e) the simplified diagram of single 3D diamondoid net in compound **3**.

btz anions. The bond distances and angles around the Ag^I ions are 2.08(3)–2.21(4) Å for Ag–N bonds and 2.64(6) Å for Ag–O bonds, while the N–Ag–N angles range is in 152.11(22)–171.07(18)°. Note that each btz ligand acts as a deprotonated tridentate anionic ligand to bridge three different Ag^I ions, almost located on a plane with the ligand btz. And the angle between the planes in which two adjacent btzs reside is 78.03(6)°. What is noteworthy in compound **3** is that there exists Ag...Ag interaction between Ag2 and Ag3, as the Ag...Ag distances (3.137 Å) are shorter than van der Waals contact distance (3.44 Å).¹⁶ The resulted basic tri-nuclear silver units (essentially acting as 4-connected nodes) play an important role in the overall 3D structural connectivity. It is connected to the four adjacent nonplanar units by two ways (Fig. 7a): (i) via coordination to POMs (which act as bi-dentate linker); (ii) through Ag–N bonds with 4,4'-bpy (Fig. S9). These eventually lead to an unprecedented diamondoid framework containing tri-nuclear silver clusters.

Interestingly, a hexa-nuclear silver-organic loop can be easily observed in this framework. The hexa-nuclear silver-organic loop is formed by two Ag1 ions, two Ag2 ions and two Ag3 ions, btz and 4,4'-bpy ligands (Fig. 7b). Further, a 1D wave chain based on the hexa-nuclear loops is constructed by sharing the Ag2 ions (Fig. 7c). The {PMo₁₂} anion can be seen as a two-connected inorganic linker by offering two terminal O atoms to link the adjacent 1D wave-like chains, leading to the final 3D net (Fig. 7d, 7e). If the hexa-nuclear loops can be simplified as bi-topic linkers, a diamondoid framework is achieved (Fig. 8a). What's more, the large void left was large enough to allow other two identical frameworks to interpenetrate the first one, leading to the whole three-fold interpenetrating structures in **3** (Fig. 8b).

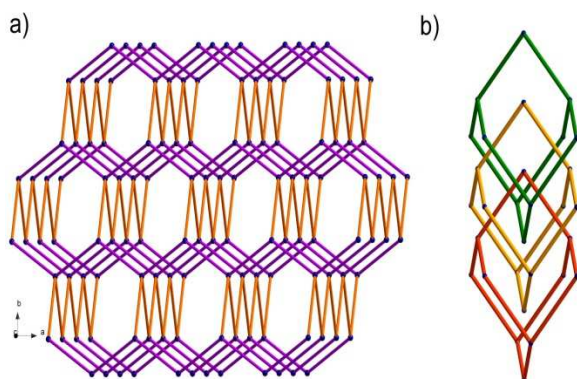


Fig. 8 Topological view of (a) single diamondoid framework and (b) three-fold interpenetrating structures in **3**.

FT-IR spectrum, XRD and TG analysis

In the IR spectrum (Fig. S3), characteristic bands of POMs are observed for $\nu(\text{P-O})$, $\nu(\text{Mo-O}_d)$, $\nu(\text{Mo-O}_b\text{-Mo})$ and $\nu(\text{Mo-O}_c\text{-Mo})$ at 1058, 954, 876, 796 cm^{-1} for **1**, 1058, 954, 869, 791 cm^{-1} for **2**, and 1061, 946, 869, 798 cm^{-1} for **3**, characteristic bands of POMs are observed for $\nu(\text{P-O})$, $\nu(\text{W-O}_d)$, $\nu(\text{W-O}_b\text{-W})$ and $\nu(\text{W-O}_c\text{-W})$ at 1083, 971, 893, 804 cm^{-1} for **4**.¹⁷ A series of bands in the region from 1143 to 1593 cm^{-1} for **1**, 1200 to 1605 cm^{-1} for **2**, 1165 to 1601 cm^{-1} for **3** and 1165 to 1600 cm^{-1} for **4** are regarded

as the bands of organic ligand Hbtz and 4,4'-bpy.

The PXRD patterns of compounds **1–4** are presented in Fig. S4. The diffraction peaks of both simulated and experimental patterns match well in the key positions, indicating the phase purities of the compounds.

TG analyses of the three compounds were carried out under N₂ atmosphere at a heating rate of 10 °C min⁻¹ in the range of 20–800 °C (Fig. S5). The weight losses of 1.29% (calc. 1.30%) in the temperature range of 20–300 °C for compound **1**, 1.40% (calc. 1.31%) in the temperature range of 20–400 °C for compound **2**, 1.80% (calc. 1.82%) in the temperature range of 20–335 °C for compound **3** and 1.41% (calc. 1.34%) in the temperature range of 20–346 °C for compound **4** are ascribed to the loss of water molecules. For compound **1**, in the temperature range of 300–700 °C, the weight loss of 16.73% (calc. 17.20%) is assigned to the release of organic ligands. The TG curve of compound **2** decreases from 400 °C until 650 °C with a weight loss of 16.87% (calc. 16.97%). For compound **3** and **4**, in the temperature range of 335–600 °C and 347–660 °C the weight loss of 19.08% (calc. 18.49%) and 13.69% (calc. 13.68%) are assigned to the release of organic ligands btz and 4,4'-bpy.

Fluorescence properties

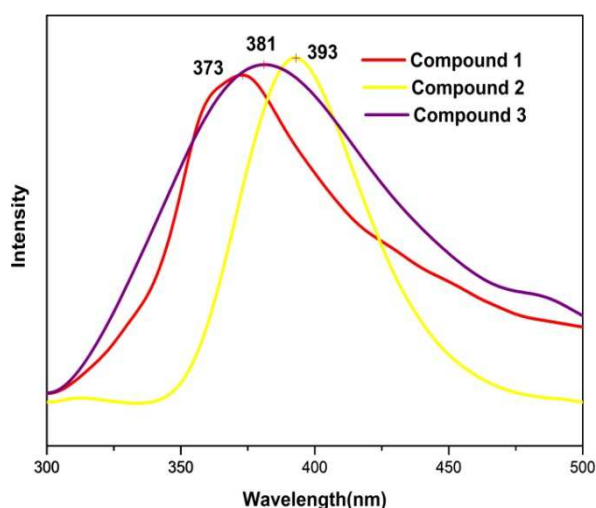


Fig. 9 Fluorescence emission spectra of compounds **1** (red), **2** (yellow) and **3** (purple) in the solid state at room temperature.

70

The solid-state luminescent properties of these hybrid compounds as well as the free Hbtz and 4,4'-bpy ligands have been investigated at room temperature. The maximal emission peaks were observed at about 373 nm ($\lambda_{\text{ex}} = 267$ nm) for **1**, 393 nm ($\lambda_{\text{ex}} = 247$ nm) for **2** and 381 nm ($\lambda_{\text{ex}} = 280$ nm) for **3** (Fig. 9). The free ligands display fluorescence properties with maximum emission peaks at 346 nm for Hbtz and 361 nm for 4,4'-bpy (Fig. S6), which could probably be ascribed to intraligand $\pi^* \rightarrow n$ or $\pi^* \rightarrow \pi$ transitions.¹⁸ Obviously, the photoluminescence spectra of compounds **1**, **2** and **3** are all red-shifted compared with the free ligands, which may be assigned to the charge-transfer transitions between ligands and metal ion centers.¹⁹ The different luminescent spectra of the title compounds may be attributed to

the different coordination environments around Ag ions. The above research implies that compounds **1**, **2** and **3** may become suitable candidates for potential inorganic-organic hybrid photoactive materials.

5 Electrochemical properties

The electrochemical behaviors of **1**-, **2**- and **3**- modified carbon paste electrodes (**1**-, **2**- and **3**-CPEs) at different scan rates were observed in 0.1 M H₂SO₄ + 0.5 M Na₂SO₄ aqueous solution. The electrochemical behaviors of the compounds **1–3** are similar except for some slight potential shift (Fig. 10 and Fig. S7), so compound **2** has been taken as an example. The cyclic voltammograms of **2**-CPE are presented in the potential range of +700 to –200 mV (Fig. 10a). There exist three reversible redox peaks I–I', II–II', and III–III' with the mean peak potentials $E_{1/2} = (E_{pa} + E_{pc})/2$ at 337 (I–I'), 135 (II–II') and –88 (III–III') mV (scan rate: 40 mV s⁻¹), respectively, which are attributed to three consecutive two-electron processes of Mo centers of PMO₁₂.²⁰ Furthermore, when the scan rate was varied from 40 to 500 mV s⁻¹, the peak potentials changed gradually: the cathodic peak potentials shift toward the negative direction and the corresponding anodic peak potentials to the positive direction

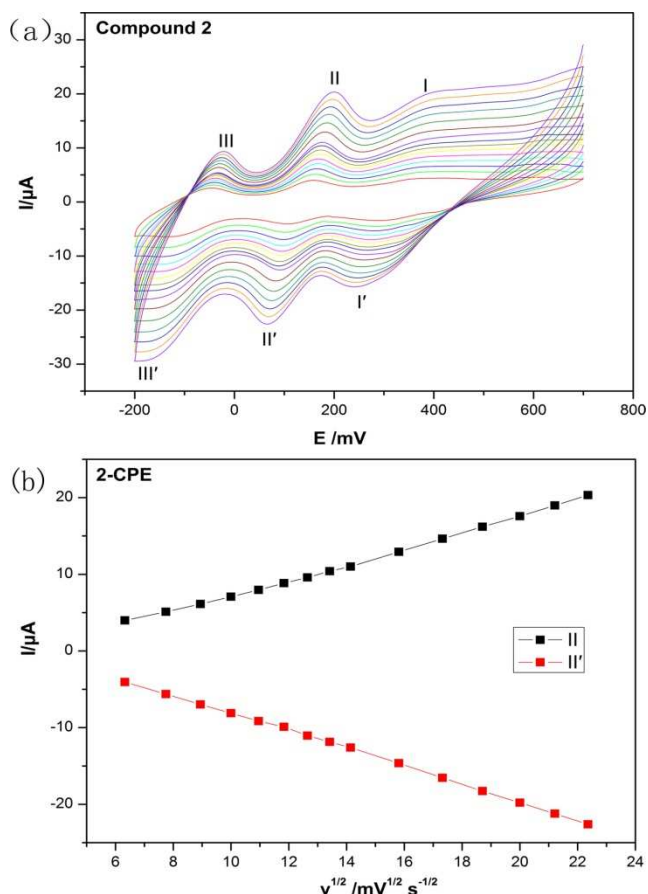


Fig. 10 (a) Cyclic voltammograms of the **2**-CPE in 0.1 M H₂SO₄ + 0.5 M Na₂SO₄ aqueous solution at different scan rates (from inner to outer: 40, 60, 80, 100, 120, 140, 160, 180, 200, 250, 300, 350, 400, 450 and 500 mV s⁻¹, respectively). (b) The dependence of anodic peak (II) and cathodic peak (II') currents of **2**-CPE on the square root of the scan rate.

with increasing scan rates. These chemically reversible processes are diffusion-controlled, as revealed by the peak current dependence on the square root of the scan rate from 40 to 500 mV s⁻¹ (Fig. 10b).²¹ As shown in Fig. S7, electrochemical processes for **1**-CPE and **3**-CPE are also diffusion-controlled. The electrochemical behaviors of **4**- modified carbon paste electrodes (**4**-CPE) at different scan rates were analysed in supporting information (Fig. S8).

UV-vis absorption spectra and optical band gap

The UV-vis absorption spectra of three hybrid compounds are presented in Fig. 11a and Fig. S9. The absorption spectra of compounds **1–3** all present one band centered around 300 nm, which is the characteristic band of polyoxometalates assigned as ligand-to-metal charge-transfer (LMCT) transition (O→Mo).²² To explore the conductivity of compounds **1–3**, the UV-vis diffuse reflectance spectra of their powder samples were tested to obtain their band gaps (E_g). The band gap, E_g , was determined as the intersection point between the energy axis and the line extrapolated from the linear portion of the absorption edge in a plot of Kubelka-Munk function F against energy E .²³ As shown in Fig. 11b and Fig. S9, the corresponding well-defined optical absorption associated with E_g can be assessed at 1.98, 2.51 and 1.96 eV for compounds **1–3**, respectively, which reveals the band gap of title compounds fall into the range of semiconductor.

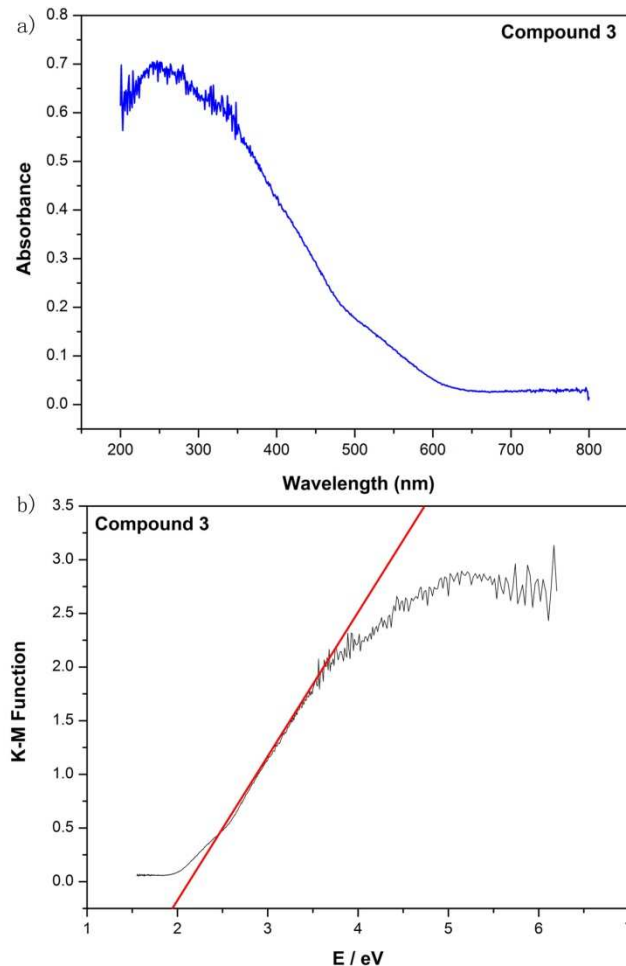


Fig. 11 (a) The diffuse reflectance UV-vis absorption spectrum of compound **3**. (b) The diffuse reflectance UV-vis-NIR spectra of K-M function vs. energy (eV) of compound **3**.

5 Conclusions

The successful syntheses for compounds **1–4** demonstrated that novel high-dimensional POMs-based hybrids frameworks can be achieved by exploiting large in-situ inorganic building blocks or proper mixed ligands. The structural diversity indicates that the combinational effects of intrinsic nature of Ag ions as well as multidentate nitrogen heterocyclic ring ligands have a significant effect on the secondary structures. While, the introduction of suitable auxiliary ligands is crucial to the final architectures of PMO₁₂-based Ag^I complexes. We believe that more high-dimensional Ag^I/POM-based hybrids can be obtained by taking advantage of the mixed ligands strategy.

Acknowledgements

We gratefully acknowledge the financial support from the NSFC of China (No. 21001022, 21171033, 21131001, 21222105, 20801041), The Foundation for Author of National Excellent Doctoral Dissertation of P. R. China (FANEDD) (No. 201022).

Notes and references

^a Institute of Functional Material Chemistry, Northeast Normal University, Changchun 130024, P. R. China. E-mail: zmsu@nenu.edu.cn.

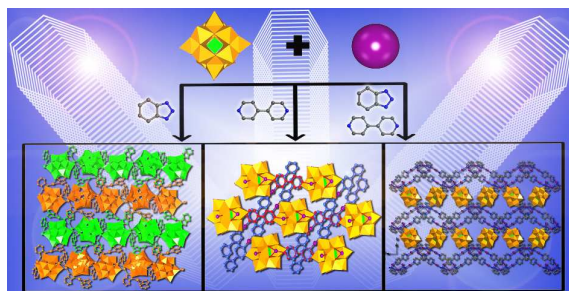
^b School of Biology and Chemistry Engineering, Jiangsu University of Science and Technology, Zhenjiang, Jiangsu 212003, P. R. China. E-mail: wangfmzj@just.edu.cn.

†Electronic Supplementary Information (ESI) available: IR Spectra, X-ray powder diffraction data, TGA plot, fluorescence properties, electrochemical properties, UV-vis absorption spectra and optical band gap and additional information. See DOI: 10.1039/b000000x/

- (a) Q. Wu, Y. G. Li, Y. H. Wang, R. Clerac, Y. Lu and E. B. Wang, *Chem. Commun.*, 2009, 5743; (b) M. A. AlDamen, S. Cardona-Serra, J. M. Clemente-Juan, E. Coronado, A. Gaita-Ariño, C. Martí-Gastaldo, F. Luis and O. Montero, *Inorg. Chem.*, 2009, 48, 3467; (c) B. Nohra, H. El Moll, L. M. Rodriguez Albelo, P. Mialane, J. Marrot, C. Mellot-Draznieks, M. O'Keefe, R. Ngo Biboum, J. Lemaire, B. Keita, L. Nadjo and A. Dolbecq, *J. Am. Chem. Soc.*, 2011, 133, 13363; (d) Y. V. Geletii, C. L. Hill, R. H. Atalla and I. A. Weinstock, *J. Am. Chem. Soc.*, 2006, 128, 17033; (e) Z. Zhou, D. Zhang, L. Yang, P. Ma, Y. Si, U. Kortz, J. Niu and J. Wang, *Chem. Commun.*, 2013, 49, 5189.
- (a) Q. Han, C. He, M. Zhao, B. Qi, J. Niu and C. Duan, *J. Am. Chem. Soc.*, 2013, 135, 10186; (b) F. J. Ma, S. X. Liu, C. Y. Sun, D. D. Liang, G. J. Ren, F. Wei, Y. G. Chen and Z. M. Su, *J. Am. Chem. Soc.*, 2011, 133, 4178; (c) C. Y. Sun, S. X. Liu, D. D. Liang, K. Z. Shao, Y. H. Ren and Z. M. Su, *J. Am. Chem. Soc.*, 2009, 131, 1883; (d) S. T. Zheng, J. Zhang and G. Y. Yang, *Angew. Chem. Int. Ed.*, 2008, 47, 3909; (e) Y. Q. Jiao, C. Qin, X. L. Wang, C. G. Wang, C. Y. Sun, H. N. Wang, K. Z. Shao and Z. M. Su, *Chem. -Asian J.*, 2014, 9, 470.
- (a) M. L. Wei, C. He, W. J. Hua, C. Y. Duan, S. H. Li and Q. J. Meng, *J. Am. Chem. Soc.*, 2006, 128, 13318; (b) J. Q. Sha, J. Peng, H. S. Liu, J. Chen, A. X. Tian and P. P. Zhang, *Inorg. Chem.*, 2007, 46, 11183; (c) J. Q. Sha, L. Y. Liang, J. W. Sun, A. X. Tian, P. F. Yan, G. M. Li and C. Wang, *Cryst. Growth Des.*, 2012, 12, 894; (d) H. Y. An, E. B. Wang, D. R. Xiao, Y. G. Li, Z. M. Su and L. Xu, *Angew. Chem. Int. Ed.*, 2006, 45, 904; (e) X. L. Wang, H. L. Hu and A. X. Tian, *Cryst. Growth Des.*, 2010, 10, 4786.
- (a) H. Y. Liu, H. Wu, J. Yang, Y. Y. Liu, J. F. Ma and H. Y. Bai, *Cryst. Growth Des.*, 2011, 11, 1786; (b) C. Y. Duan, M. L. Wei, D. Guo, C. He and Q. J. Meng, *J. Am. Chem. Soc.*, 2009, 132, 3321; (c) P. Mialane, A. Dolbecq, L. Lisnard, A. Mallard, J. Marrot and F. Sécheresse, *Angew. Chem. Int. Ed.*, 2002, 41, 2398; (d) M. L. Qi, K. Yu, Z. H. Su, C. X. Wang, C. M. Wang, B. B. Zhou and C. C. Zhu, *Dalton Trans.*, 2013, 42, 7586; (e) Y. Q. Jiao, C. Qin, X. L. Wang, F. H. Liu, P. Huang, C. G. Wang, K. Z. Shao and Z. M. Su, *Chem. Commun.*, 2014, DOI: 10.1039/c3cc47703g, in press.
- (a) A. X. Tian, J. Ying, J. Peng, J. Q. Sha, Z. M. Su, H. J. Pang, P. P. Zhang, Y. Chen, M. Zhu and Y. Shen, *Cryst. Growth Des.*, 2010, 10, 1104; (b) A. X. Tian, J. Ying, J. Peng, J. Q. Sha, H. J. Pang, P. P. Zhang, Y. Chen, M. Zhu and Z. M. Su, *Cryst. Growth Des.*, 2008, 8, 3717; (c) M. G. Liu, P. P. Zhang, J. Peng, H. X. Meng, X. Wang, M. Zhu, D. D. Wang, C. L. Meng and K. Alimaje, *Cryst. Growth Des.*, 2012, 12, 1273; (d) K. Uehara, T. Oishi, T. Hirose and N. Mizuno, *Inorg. Chem.*, 2013, 52, 11200.
- (a) X. F. Kuang, X. Y. Wu, R. M. Yu, J. P. Donahue, J. S. Huang and C. Z. Lu, *Nat. Chem.*, 2010, 2, 461; (b) H. Yang, S. Gao, J. Lu, B. Xu, J. Lin and R. Cao, *Inorg. Chem.*, 2010, 49, 736; (c) X. Kuang, X. Y. Wu, J. Zhang and C. Z. Lu, *Chem. Commun.*, 2011, 47, 4150.
- (a) C. Streb, C. Ritchie, D. L. Long, P. Kogerler and L. Cronin, *Angew. Chem. Int. Ed.*, 2007, 46, 7579; (b) P. P. Zhang, J. Peng, H. J. Pang, J. Q. Sha, M. Zhu, D. D. Wang, M. G. Liu and Z. M. Su, *Cryst. Growth Des.*, 2011, 11, 2736; (c) H. Y. An, Y. G. Li, E. B. Wang, D. R. Xiao, C. Y. Sun and L. Xu, *Inorg. Chem.*, 2005, 44, 6062.
- (a) P. Mialane, A. Dolbecq and F. Sécheresse, *Chem. Commun.*, 2006, 3477; (b) Y. Q. Lan, S. L. Li, Z. M. Su, K. Z. Shao, J. F. Ma, X. L. Wang and E. B. Wang, *Chem. Commun.*, 2008, 58; (c) J. L. Xie, B. F. Abrahams and A. G. Wedd, *Chem. Commun.*, 2008, 576; (d) S. L. Li, Y. Q. Lan, J. F. Ma, J. Yang, J. Liu, Y. M. Fu and Z. M. Su, *Dalton Trans.*, 2008, 2015.
- (a) Z. B. Han, G. Y. Luan and E. B. Wang, *Transition Met. Chem.*, 2003, 28, 63; (b) X. L. Wang, Y. F. Wang, G. C. Liu, A. X. Tian, J. W. Zhang and H. Y. Lin, *Dalton Trans.*, 2011, 40, 9299.
- (a) C. Inman, J. M. Knaust and S. W. Keller, *Chem. Commun.*, 2002, 156; (b) L. L. Fan, D. R. Xiao, E. B. Wang, Y. G. Li, Z. M. Su, X. L. Wang and J. Liu, *Cryst. Growth Des.*, 2007, 7, 592; (c) J. Q. Sha, J. Peng, A. X. Tian, H. S. Liu, J. Chen, P. P. Zhang and Z. M. Su, *Cryst. Growth Des.*, 2007, 7, 2535; (d) C. Z. Lu, C. D. Wu, H. H. Zhuang and J. S. Huang, *Chem. Mater.*, 2002, 14, 2649.
- D. D. Wang, J. Peng, H. J. Pang, P. P. Zhang, X. Wang, M. Zhu, Y. Chen, M. G. Liu and C. L. Meng, *Inorg. Chim. Acta*, 2011, 379, 90-94.
- H. T. Evans and M. T. Pope, *Inorg. Chem.*, 1984, 23, 501.
- L. S. Wang, P. C. Yin, J. Zhang, J. Hao, C. L. Lv, F. P. Xiao and Y. G. Wei, *Chem. Eur. J.*, 2011, 17, 4796-4801.
- (a) X. L. Wang, C. Qin, E. B. Wang, Z. M. Su, Y. G. Li and L. Xu, *Angew. Chem. Int. Ed.*, 2006, 45, 7411-7414; (b) Q. G. Zhai, X. Y. Wu, S. M. Chen, Z. G. Zhao and C. Z. Lu, *Inorg. Chem.*, 2007, 46, 5046.
- J. X. Chen, T. Y. Lan, Y. B. Huang, C. X. Wei, Z. S. Li and Z. C. Zhang, *J. Solid State Chem.*, 2006, 179, 1904-1910.
- P. Pyykkö, *Chem. Rev.*, 1997, 97, 597.
- R. Thouvenot, M. Fournier, R. Franck and C. Rocchiccioli-Deltcheff, *Inorg. Chem.*, 1984, 23, 598.
- J. Guo, J. Yang, Y. Y. Liu and J. F. Ma, *Inorg. Chim. Acta*, 2013, 400, 51.
- X. G. Liu, L. Y. Wang, X. Zhu, B. L. Li and Y. Zhang, *Cryst. Growth Des.*, 2009, 9, 3997.
- X. L. Hao, Y. Y. Ma, C. Zhang, Q. Wang, X. Cheng, Y. H. Wang, Y. G. Li and E. B. Wang, *CrystEngComm*, 2012, 14, 6573.
- P. I. Molina, H. N. Miras, D. L. Long and L. Cronin, *Inorg. Chem.*, 2013, 52, 9284.
- S. L. Zhao, H. H. Zhang and C. C. Huang, *Chem. J. Chin. Univ.*, 2002, 23, 521.
- J. I. Pankove, *Optical Processes in Semiconductors*; Prentice-Hall: Englewood Cliffs, NJ, 1971; p 34.

Syntheses, crystal structures and properties of inorganic-organic hybrids constructed from Keggin-type polyoxometalates and silver coordination compounds†

Wei-Li Zhou,^a Jun Liang,^a Chao Qin,^{*a} Kui-Zhan Shao,^a Fang-Ming Wang^{*b} and Zhong-Min Su^{*a}



Four high-dimensional Ag^I/POM-based hybrids have been synthesized and their optical band gaps, electrochemical and fluorescence properties have been investigated.